High strain-rate deformation fabrics characterize a kilometers-thick Paleozoic fault zone in the Eastern Sierras Pampeanas, central Argentina

Steven J. Whitmeyer[*], Carol Simpson

Department of Earth Sciences, Boston University, Boston, MA 02215, USA

Abstract

High strain rate fabrics that transgress a crustal depth range of ca. 8–22 km occur within a major Paleozoic fault zone along the western margin of the Sierras de Córdoba, central Argentina. The NNW-striking, east-dipping 'Tres Arboles' fault zone extends for at least 250 km and separates two metamorphic terranes that reached peak temperatures in the middle Cambrian and Ordovician, respectively. Exposed fault zone rocks vary from a 16-km-thickness of ultramylonite and mylonite in the southern, deepest exposures to <5 km in the northern, shallower-level exposures.

Three transects across the fault zone have been examined in detail. In the deepest section, newly crystallized sillimanite needles define the foliation and wrap garnet and feldspar theta- and delta-type porphyroclasts in a biotite-rich ultramylonite. Geothermometry and preserved microstructures in feldspar and quartz indicate deformation at temperatures >520 °C. Reaction-enhanced grain size reduction and grain boundary sliding were the predominant deformation mechanisms in these high strain rate rocks. Ultramylonites in the intermediate depth section also contain evidence for grain boundary sliding and diffusional mass transfer, although overprinted by late stage chlorite. In the shallowest exposed section, rocks were deformed at or near to the brittle–ductile transition to produce mylonite, cataclasite, shear bands and pseudotachylyte.

The overall structure of the Tres Arboles zone is consistent with existing fault zone models and suggests that below the brittle–ductile transition, strain compatibility may be accommodated through very thick zones of high temperature ultramylonite.
© 2002 Elsevier Science Ltd. All rights reserved.

Keywords: Sierras Pampeanas; 'Tres Arboles' fault zone; Amphibolite facies dutile deformation

1. Introduction

An extensive body of research exists on experimentally and naturally deformed mylonitic and ultramylonitic rocks. The bulk of this work has concentrated on greenschist- to lower amphibolite-facies deformation (e.g. Bell and Etheridge, 1973; Tullis, 1977; Knipe, 1989), and only recently has field-based research broadened to include higher-grade zones of ductile deformation. A result of this historical preoccupation with low-grade mylonites is the common perception that ductile deformation is concentrated into narrow, strain-localizing zones. This interpretation is supported by the brittle–ductile transition region of Sibson's continental fault zone model (Sibson, 1977, 1986), where shear zones are described as planar, parallel-sided strain-concentrating bands of protomylonite to mylonite. However, with increased depth and temperature, this model predicts that shear resistance in the host rocks decreases, resulting in more homogenous strain fabrics across a thickened deformation zone (Sibson, 1977, 1986; Scholz, 1990). The implication is that deep-crustal shear zones should feature impressive thicknesses of amphibolite- to granulite-facies deformation fabrics, in distinct contrast to the well-documented, localized greenschist-facies mylonites of higher structural levels.

There are relatively few documented examples of kilometer-scale shear zones consisting almost exclusively of amphibolite and higher-grade mylonite and ultramylonite. In the Archean–Proterozoic tectonic belts of North America, greenschist to granulite facies ductile shear zones separate the three principal belts of the 0.9–1.5 Ga Grenville Orogen, which stretches 2000 km from northern New York to Labrador (Davidson, 1986). In the Grenville Front tectonic zone, granulite to amphibolite facies

* Corresponding author. Tel.: +1-617-358-1108; fax: +1-617-353-3290.
E-mail address: stevenw@bu.edu (S.J. Whitmeyer).
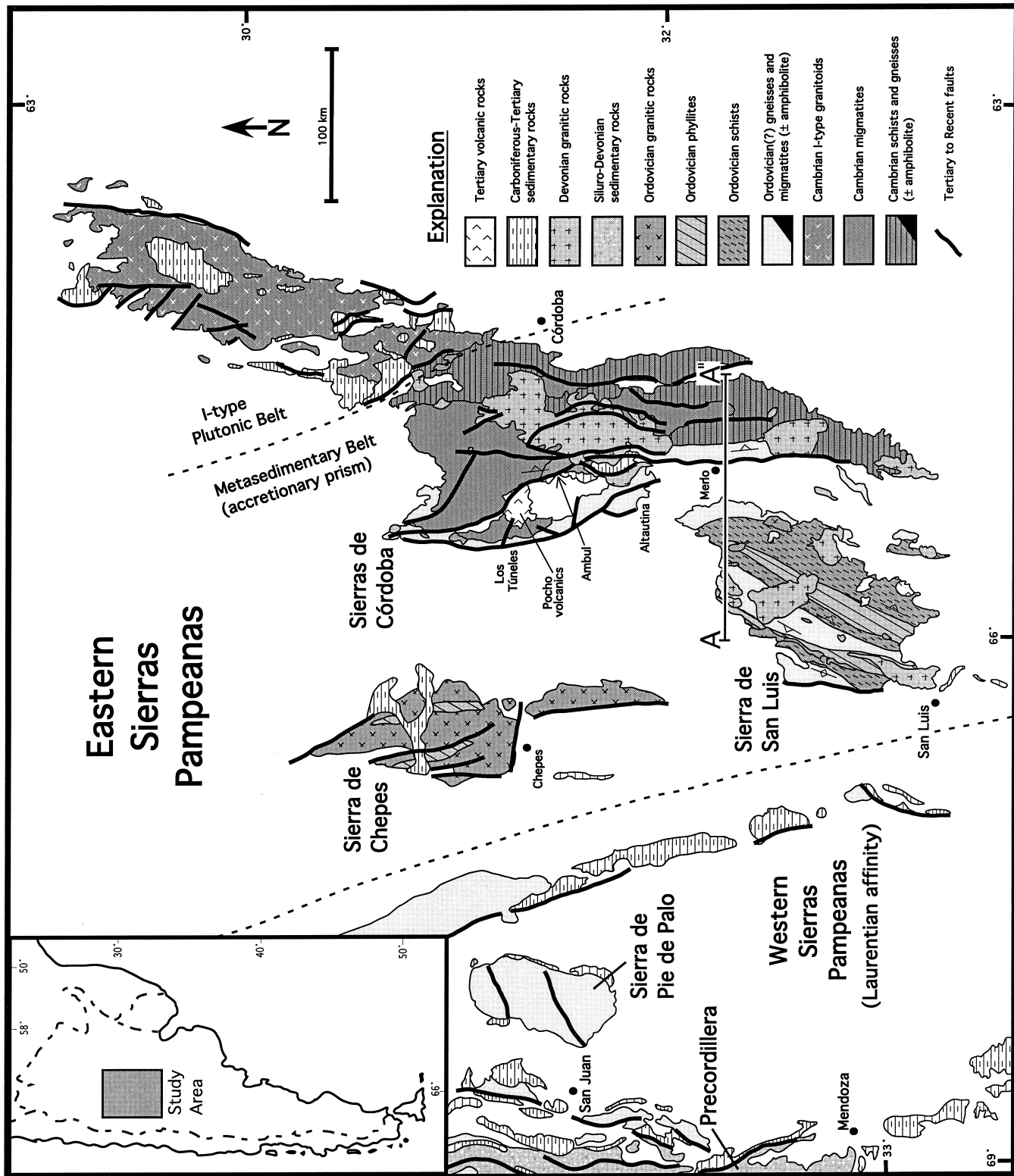
mylonites and ultramylonites predominate along the kilo-meters-wide boundary between the Grenville Province and the Superior Province to the NW (Davidson, 1990; Gower and Simpson, 1992). Granulite facies mylonite belts reach a thickness of 5–10 km in Archean cratonic sutures within the Snowbird tectonic zone (Hanmer and Kopf, 1993; Hanmer et al., 1995). However, Paleozoic and younger high strain zones of continental-scale importance are generally exposed at higher structural levels than those in the older rocks, and thus the preserved deformation features that have been studied from large high strain zones were generally formed at greenschist and lower metamorphic facies.

In this paper we present data from an extensive early Paleozoic ductile shear zone located in the Eastern Sierras Pampeanas of central Argentina, where migmatites and sillimanite-grade metasedimentary rocks are juxtaposed against lower-grade metapsammites and metapelites across a zone of amphibolite to upper greenschist facies ultra-mylonite and mylonite. The significance of this 16-km-thick zone of high strain and high strain-rate rocks is examined in terms of the dominant deformation mechanisms and the implied tectonic environment.

2. Tectonic setting

The Eastern Sierras Pampeanas of north-central Argen-tina, comprising the Sierras de Córdoba in the east and the Sierra de San Luis to the southwest (Fig. 1), are a system of north–south basement uplifts separated by deep, asymme-trical, sediment-filled valleys. Exposure of Cambrian I-type plutons and associated metasedimentary rocks in the uplifts occurred on high-angle, Tertiary to Recent reverse faults (Jordan and Allmendinger, 1986). The metasedimentary rocks are interpreted as originally part of an early Cambrian accretionary prism that formed along the western Gond-wana convergent margin (Dalla Salda et al., 1992a; Dalziel et al., 1994; Dalziel, 1997; Lyons et al., 1997; Northrup et al., 1998; Rapela et al., 1998a). Rapela et al. (1998b) and Gromet and Simpson (1999) obtained ca. 520 Ma ages for migmatization in the Sierras de Córdoba, which represents the peak metamorphic event within the Córdoba ranges (see also Pérez et al., 1996; Rapela et al., 1998a; Stuart-Smith et al., 1999).

Oblique convergence along the developing PaleoPacific margin of Gondwana facilitated the accretion of the Laurentia-affiliated Precordillera terrane outboard of the Sierras Pampeanas during the Ordovician Famatinian Orogeny (Dalla Salda et al., 1992a,b; Pankhurst et al., 1996). Ordovician peak metamorphism and plutonism is documented across the central and eastern regions of the Sierra de San Luis, where zircons and monazites from high-

grade schists and gneisses yield ages of 460–485 Ma (Camacho and Ireland, 1997; Sims et al., 1997, 1998; Stuart-Smith et al., 1999; Gromet et al., 2001; von Gosen et al., 2002; Gromet, personal communication).
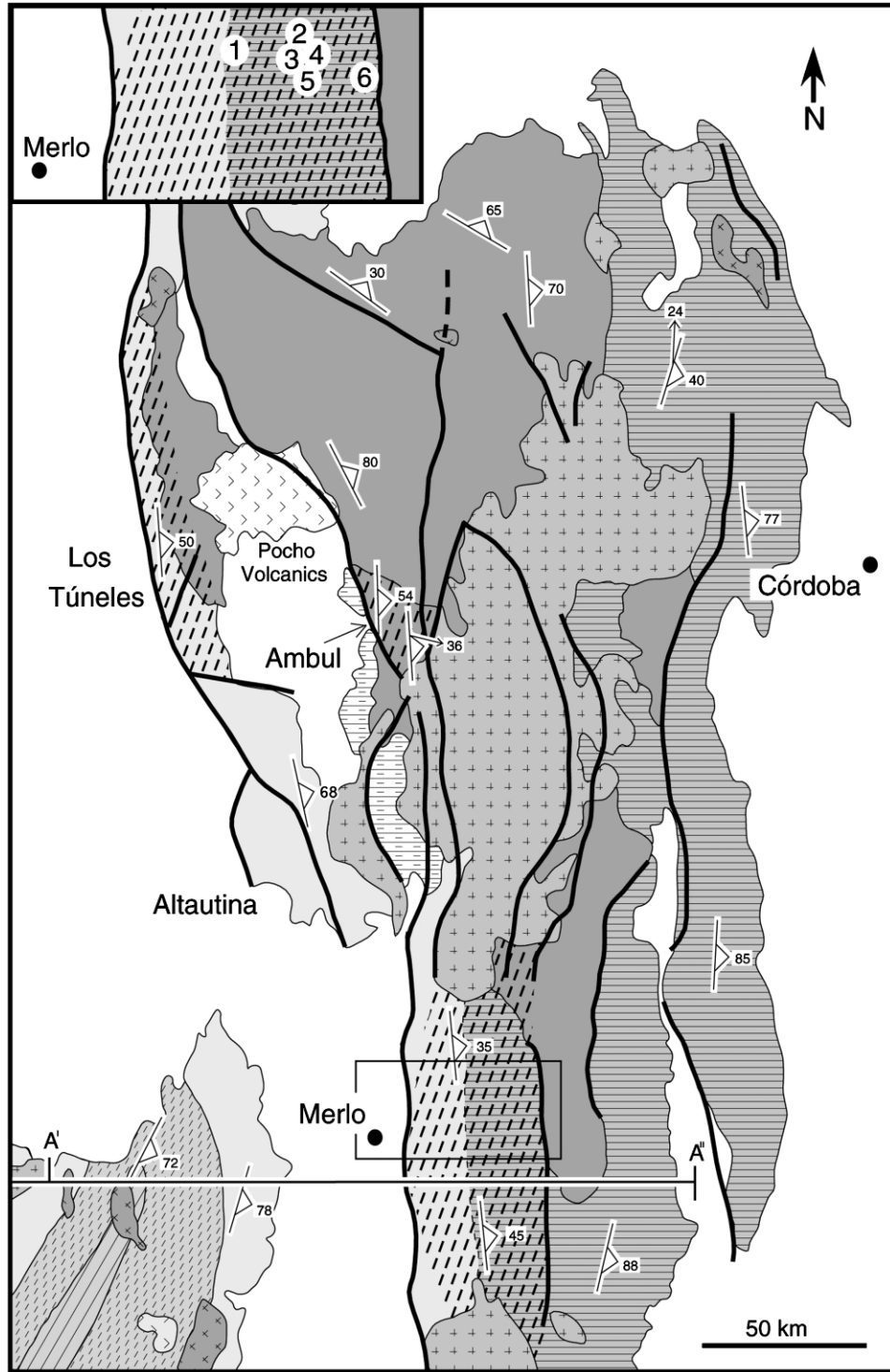
Ordovician to Devonian ductile faulting occurred in meter- to hundred meter-scale shear zones throughout the Eastern Sierras Pampeanas. Many of these mylonite and ultramylonite zones thrust sillimanite grade gneisses, migmatites and schists westward over biotite to chlorite grade phyllites. The most significant of these ultramylonite zones, called here the 'Tres Arboles' fault zone, juxtaposed the Cambrian and Ordovician metamorphic terranes and now extends NNW along the western margin of the Sierras de Córdoba for at least 150 km (Fig. 2), locally reaching 16 km in thickness. The zone is tilted down along strike to the north, as are all structures within the Sierras de Córdoba (Cerredo, 1996; Otamendi and Rabbia, 1996; Northrup et al., 1998), which exposes a section of approximately 10 km depth through the fault-related rocks. Descriptions of the macro- and micro-fabrics from within each of three structural depth sections of the fault zone follow.

3. The Tres Arboles fault zone

3.1. Deepest section (Merlo region)

Hanging wall rocks east of and proximal to the Tres Arboles fault zone in the vicinity of Merlo (Fig. 2) include biotite + sillimanite + garnet ± cordierite schists and gneisses with large areas of interfingered potassium feldspar-rich migmatite (Figs. 2 and 3). Schists and gneisses outside the high strain zone contain abundant quartz and pegmatitic stringers that are typically folded and boudi-naged (Fig. 4a). Small-scale, tight, west-vergent folds are locally apparent, but have not yet been found on the regional scale. Zones of migmatitic granite are intermingled with gneissic xenoliths and are thought to result from localized in-situ melting at 2nd sillimanite grade. Within the migmatites, peak metamorphic temperatures and pressures of 650–950 °C and 6.5–8 kbar (Gordillo, 1984; Otamendi et al., 1999) were reached at 520–535 Ma (U–Pb ages for metamorphic monazite; Gromet and Simpson, 1999).

The footwall of the Tres Arboles fault zone comprises mainly quartz + feldspar + biotite psammites, with associ-ated biotite + muscovite schists and phyllites (the Conlara Metamorphic Complex of Sims et al. (1997); Figs. 2 and 3). Footwall foliations are oriented roughly parallel to NNW-striking, east-dipping axial surfaces of regional folds. The psammites contain an early pressure solution cleavage and buckled quartz veins (Fig. 4b); nearby biotite schists contain buckled quartz–feldspar veins. Localized quartz +

Fig. 1. Simplified geologic map of the Eastern Sierras Pampeanas. Modified from Lucero Michaut et al. (1995).

Explanation

Tertiary volcanic rocks	Ordovician phyllites
Carboniferous-Tertiary sedimentary rocks	Ordovician schists
Devonian granitic rocks	Ordovician(?) gneisses and migmatites (± amphibolite)
Ordovician granitic rocks	Cambrian migmatites

Cambrian schists and gneisses (± amphibolite)	
Tertiary to Recent faults	
Tres Arboles shear zone	
Strike and dip of foliation	

Table 1
Thickness calculation for regions of Tres Arboles fault zone

Region	Horizontal width of sheared rocks	Average dip of mylonitic foliations	Calculated thickness of shear zone
Merlo	20 km	55°E	16 km
Ambul	10 km	35°E	6 km (minimum)
Los Túneles	3 km	50°NE	2 km (minimum)

feldspar ± tourmaline pegmatites, discontinuous veins of biotite granite and local migmatites are increasingly abundant adjacent to the Tres Arboles fault zone. Recent U–Pb dating of metamorphic monazite grains from unsheared gneissic psammites in the footwall provide an age of 453 ± 2 Ma (Gromet, personal communication), consistent with the regional mid-Ordovician heating event in the footwall prior to initiation of the Tres Arboles shear zone.

The Merlo section of the Tres Arboles fault zone contains 16 km thickness of amphibolite facies ultramylonitic and mylonitic rocks (Table 1), with only minor amounts of protomylonite. Mylonitic footwall psammites containing lenses of relatively low strain predominate across the western 4–5 km of the fault zone. Deformation intensity is generally greatest in the central and eastern, structurally higher, part of the fault zone section where hanging wall sillimanite gneisses and schists are incorporated. Mineral lineations and foliations in the eastern ultramylonites are poorly defined in outcrop (Fig. 4c); the majority have 30–50° east to southeast dips with a down dip lineation, where present (Fig. 5a). Samples containing euhedral, equilibrated, pre- to early-syntectonic garnet, biotite and sillimanite were collected from sheared hanging wall rocks along a transect from the middle of the fault zone eastward to the undeformed gneisses and migmatites. Preliminary results from garnet–biotite geothermometry yield temperatures between 540 and 590 °C at pressures of approximately 3–6 kbar (Table 2; Fig. 6). At present, appropriate mineral assemblages for geothermometry have not been identified within the sheared footwall rocks.

3.2. Intermediate depth section (Ambul region)

A presumed continuation of the Tres Arboles fault zone extends for 20 km north of the 368 ± 2 Ma (U–Pb zircon; Dorais et al., 1997) Achala batholith in the Ambul region (Fig. 2), where a 15-km-wide zone of ultramylonite and interspersed mylonite is truncated on its eastern and western margins by Tertiary brittle faults. Ultramylonites in the region lack a strong foliation or lineation, and foliations are usually apparent only in mylonitic granitoids and quartz veins (Fig. 4d), where they strike predominantly NNW and

dip 30–50° NE. Stretching lineations even in mylonites are poorly defined, but those in evidence mostly plunge down-dip (Fig. 5b). Occasional S/C mylonites with mica fish show east over west movement. Although not observed on a regional scale, localized, small, dextral strike slip zones occur in the Ambul region and just north of the Los Túneles area (Fig. 2).

3.3. Shallowest section (Los Túneles region)

Intermingled ductile and brittle fault structures crop out for at least 100 km along strike on the northwest margin of the Sierras de Córdoba (Simpson et al., 2001; Fig. 2). In the Los Túneles region, steeply east-dipping sillimanite-grade gneisses and migmatites (Gordillo, 1984) are thrust to the west over kinked and pressure-solved chlorite-grade phyllites. The southeastern extension of the Los Túneles zone is truncated by normal faults related to Cretaceous and younger basin development and the intrusion of the Tertiary Pocho volcanic edifice (Kay and Gordillo, 1994); however, restoration of the Tertiary extension would situate the Los Túneles zone along strike with the Ambul zone. Regional foliations outside the fault zone strike NNW and dip at 60–80° ENE (Fig. 2).

The fault zone in this region contains a several hundred meter thick zone of shear bands, narrow zones of mylonite and ultramylonite, and associated cataclasites and pseudo-tachylyte. Mylonites and ultramylonites contain elongate quartz ribbons and sigma- and delta-grain feldspar porphyr-oclasts. These are overprinted by 5–10 cm spaced, east-dipping biotite- and chlorite-grade shear bands that clearly demonstrate east over west movement (Fig. 4e). Orientations of the C planes are tightly clustered, with predominantly NNW strikes and generally moderate but variable dips of 30–50° NE; stretching lineations are predominantly down-dip (Fig. 5c). Chlorite retrogression of the shear banded rocks is more pervasive structurally lower in the section, close to a sharply delineated younger brittle thrust contact with the underlying phyllites. For a vertical distance of 100 m directly above the thrust contact, the zone also contains ultracataclasite and abundant centimeter-thick pseudotachylyte veins.

Fig. 2. Enlargement of Fig. 1 showing the detailed geology of the northeastern region of the Sierra de San Luis and the central and northern areas of the Sierras de Córdoba. Note the three regions of the Tres Arboles fault zone near Merlo, Ambul and Los Túneles. Region defined by rectangular box near Merlo is enlarged in the upper left and shows locations of samples used for geothermometry (numbers in white circles).
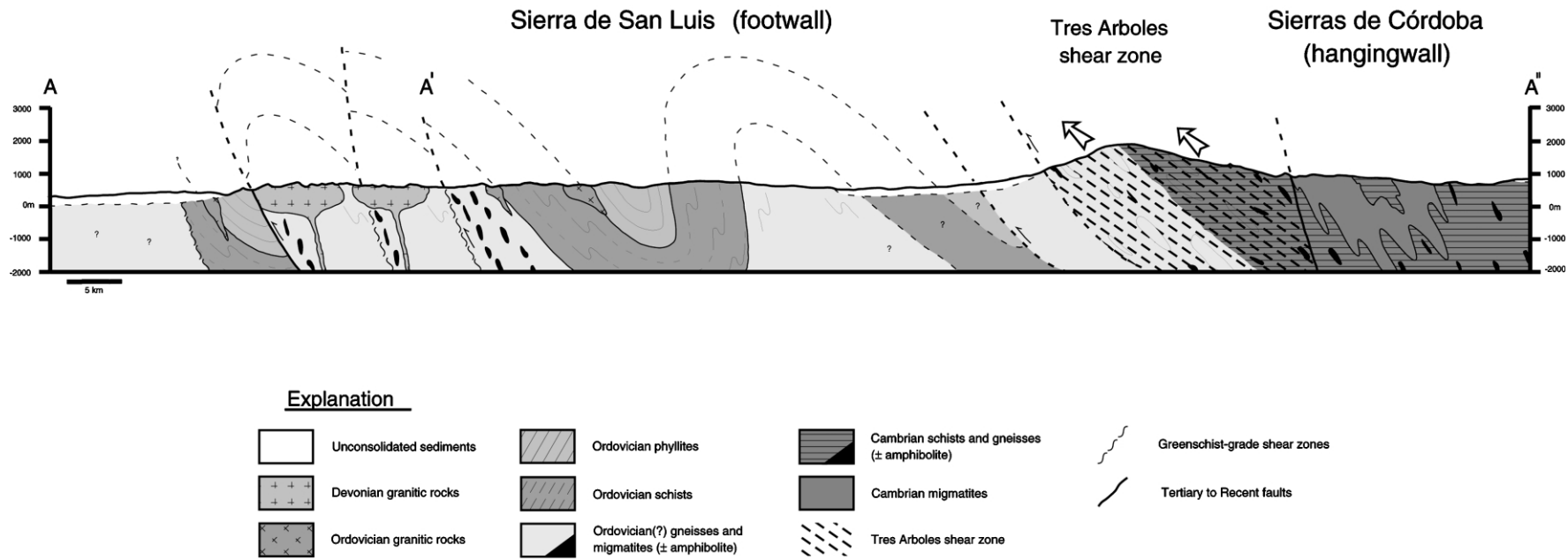
Fig. 3. Geologic cross-section along the transect defined by A–A″ in Fig. 1, and A′–A″ in Fig. 2. Note the change in scale.
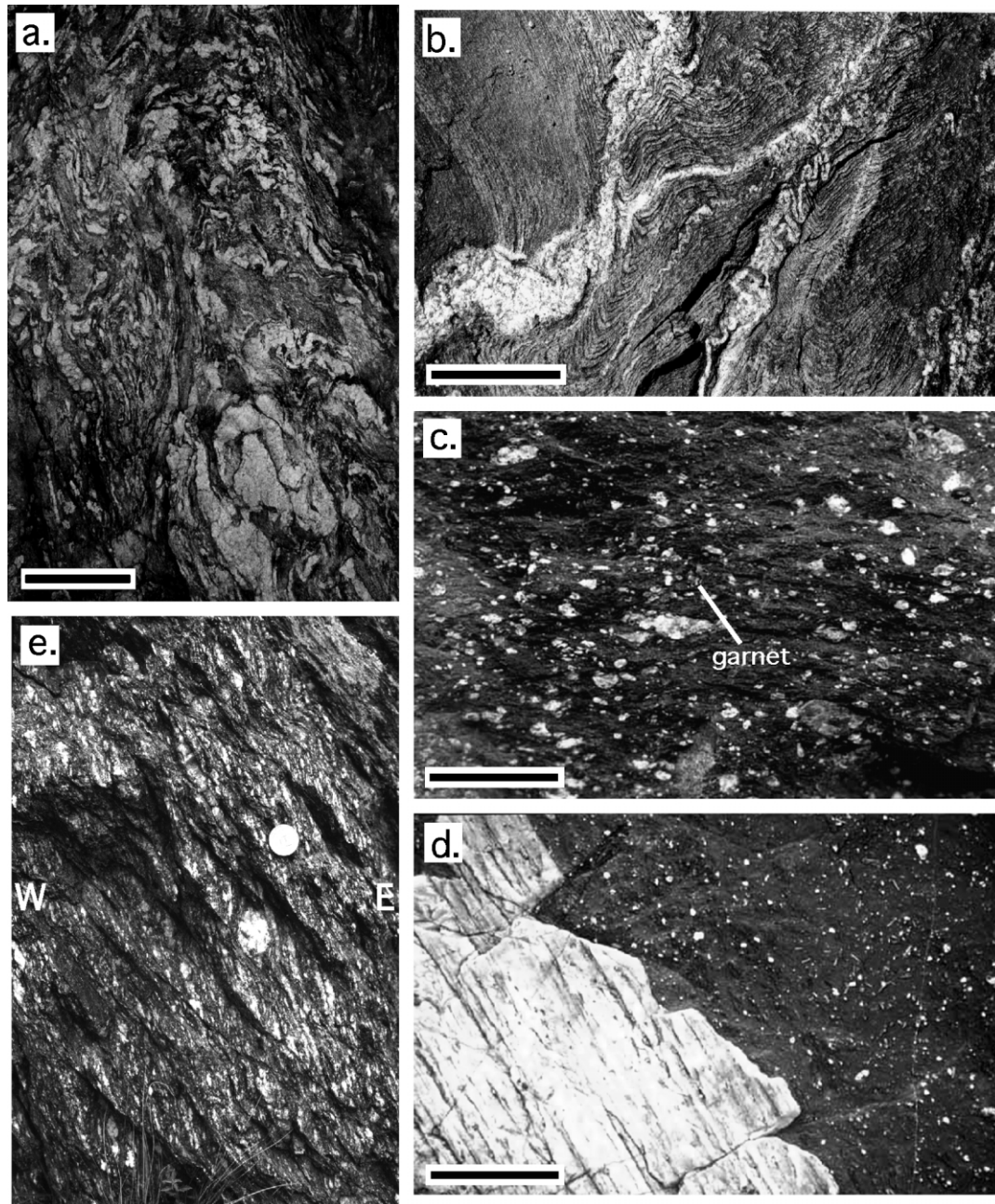
Fig. 4. (a) Outcrop of folded and partially migmatized garnet + sillimanite gneiss in the hanging wall east of the Tres Arboles shear zone. (b) Outcrop of folded and partially migmatized biotite psammite from the unsheared footwall west of the Tres Arboles shear zone. (c) Ultramylonite derived from garnet–biotite–sillimanite gneiss of the hanging wall. (d) Outcrop of mylonitic quartz vein with strong lineation (white, at left), within poorly foliated and lineated ultramylonite zone in Ambul area, northwest of Achala batholith. View down onto foliation plane. (e) Los Túneles shear bands showing east over west movement. Coin diameter for (e) = 2 cm; scale bars for (a), (c) = 3 cm; (b), (d) = 5 cm.

4. Microstructures

4.1. Merlo region

In the deepest exposed section of the Tres Arboles fault zone near Merlo, biotite + garnet + sillimanite ultramylonites that are closest to the hanging wall of the zone contain euhedral, 5–15 μm sillimanite needles that define the lineation within a <5 μm matrix of biotite + quartz + feldspar (Fig. 4c). The sillimanite needles display minimal fracturing with little or no boudinage (Fig. 7a). Coarser-grained (200–500 μm) relict sillimanite is also present, either as isolated fragments or as stretched and boudinaged grains, often mantled by much finer-grained, secondary-growth fibrolite. Quartz predominantly occurs as elongate ribbons with subgrains and fully recovered, strain-free, polygonal grains indicative of Regime II to Regime III recrystallization (Hirth and Tullis, 1992).
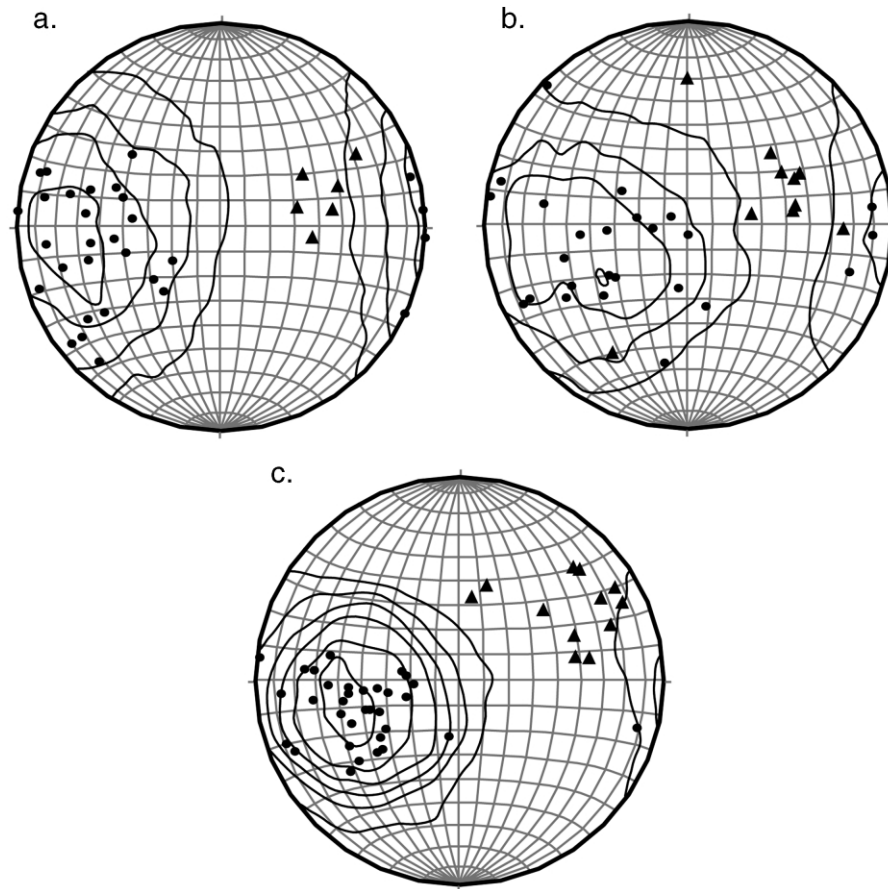
Fig. 5. Lower hemisphere stereographic projections of poles to mylonitic foliations (bullet) with 1% area contours, and trend and plunge of stretching lineations (triangle) in Tres Arboles fault zone. (a) Merlo region, (b) Ambul region, (c) Los Túneles region.

Within narrow zones of finer grained and apparently lower temperature hanging wall ultramylonites, the biotite-rich matrix has a grain size of < 3 μm and shows a weak preferred orientation that defines a poorly developed foliation. 200–400 μm diameter feldspar porphyroclasts are typically round to elliptical, often without recrystallized tails (theta-type grains; Hooper and Hatcher, 1988) and with largely undeformed interiors (Fig. 7b). Narrow bands of fine-grained (< 5 μm) recrystallized feldspar frequently mantle the porphyroclasts; occasional porphyroclasts exhibit core and mantle structures, consistent with Regime I to lower Regime II recrystallization in feldspar (Hirth and

Table 2
Garnet–biotite geothermometry of sheared hanging wall samples, using method of Holdaway (2000). Sample (1) is from center of fault zone; samples (2)–(5) are from eastern half of fault zone; sample (6) is from eastern margin of fault zone

Sample	Pressure range	Temperature range (± 25 °C 2Σ absolute error)
1	3.1–5.3 kbar	560–565 °C
2	3.4–4.9 kbar	540–545 °C
3	3.2–5.2 kbar	555–560 °C
4	2.8–5.8 kbar	575–590 °C
5	3.4–4.8 kbar	540–545 °C
6	2.9–5.6 kbar	575–580 °C

Tullis, 1992). Reaction products of white mica + quartz around the rims of some feldspar porphyroclasts locally produce very fine-grained 'tails' (Fig. 7b). Relict 150–200 μm garnet clasts typically include undeformed 10–25 μm biotite grains and may be surrounded by ≤5-μm-thick rims of newly precipitated quartz. In general, shear sense is difficult to resolve within the ultramylonitic rocks due to a lack of diagnostic features, but where present, sigma- and delta-type porphyroclasts display east over west movement.

Psammitic mylonites and ultramylonites closest to the footwall contain abundant feldspar porphyroclasts, but preserve relatively few coarse biotite clasts from the protolith rocks. Neither garnet nor sillimanite has been found in the footwall-derived mylonites. Elongate quartz ribbons exhibit deformation bands and subgrains with equant rotation-recrystallized grains (Fig. 7c), which are consistent with Regime II recrystallization. Internally strain-free 100–200 μm feldspar porphyroclasts reveal fine-grained reaction rims of white mica + quartz and tails of very fine-grained recrystallized feldspar (Fig. 7c). Granitic mylonites at the base of the fault zone typically have an S/C fabric with shear bands defined by stable muscovite + biotite ± chlorite that exhibit minor kinks and evidence for sliding along basal 001 planes. Quartz
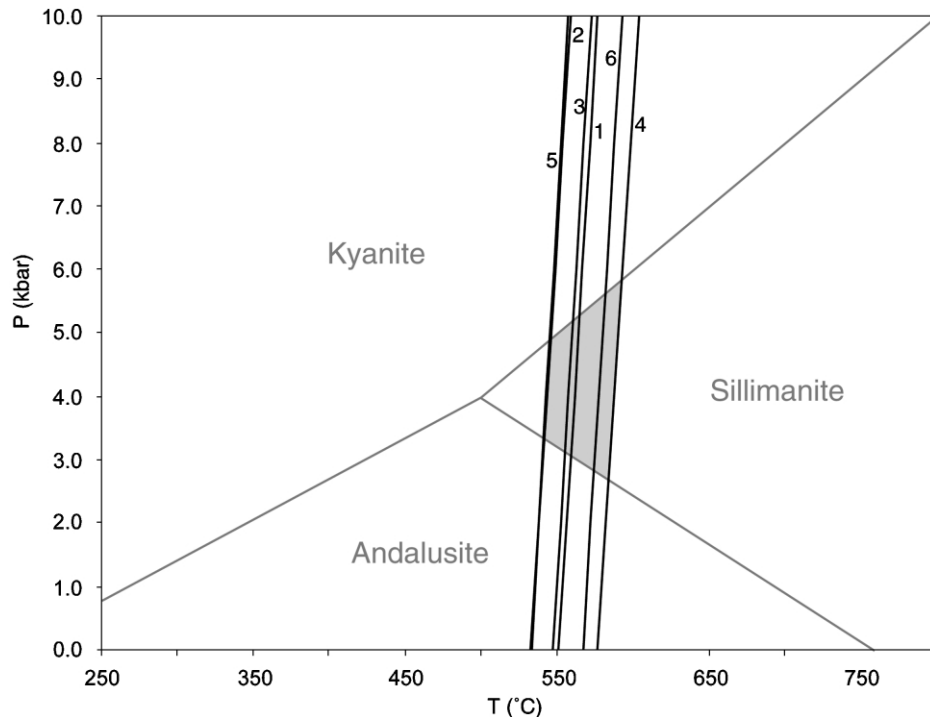
Fig. 6. Garnet–biotite geothermometry of six samples of sillimanite-bearing hanging wall schists and gneisses across a west to east transect from center of Merlo fault zone to eastern margin of fault zone. Sample (1) is from center of fault zone; samples (2)–(5) are from eastern half of fault zone; sample (6) is from eastern margin of fault zone. Shaded area represents pressure and temperature range during deformation of hanging wall rocks. Geothermometer from Holdaway (2000), see Table 2 for data.

aggregates in the S/C mylonites are elongate and contain subgrains and recrystallized equant grains with straight boundaries consistent with Regime II recrystallization. Feldspar porphyroclasts contain minor intergranular fractures and kinks with sutured grain boundaries, indicative of grain boundary migration recrystallization along grain margins. Sigma- and delta-grains, where present, clearly demonstrate east over west movement.

4.2. Ambul region

Ultramylonites in the Ambul region are very similar in microstructure to those closest to the footwall in the Merlo transect. Porphyroclasts from the biotite + chlorite ultramylonites in the Ambul zone show little internal deformation; garnets often have narrow quartz rims, and feldspars are bordered by reaction rims of quartz + white mica, occasionally with recrystallized tails (Fig. 7d). Porphyroclasts occur in a $<10\ \mu m$ matrix of chlorite + biotite + quartz. Occasionally, quartz occurs in elongate ribbons with subgrains and equant, rotational-recrystallized grains, indicative of Regime II recrystallization. Fine grained sillimanite needles are present in some samples, typically with partial alteration to white mica; needles are elongated parallel to the foliation and help define the lineation. The ultramylonitic matrix contains randomly oriented, very fine-grained ($<2\ \mu m$) chlorite and biotite

that overgrows and partially obscures an earlier foliation. We interpret this chlorite growth to be a later greenschist-grade phase of retrogression, unrelated to the Tres Arboles fault deformation.

4.3. Los Túneles region

Ductile deformation fabrics in the hanging wall section of the Los Túneles zone include mid- to upper-greenschist-grade mylonites and protomylonites that contain elongate feldspar porphyroclasts with sutured grain boundaries and small newly-recrystallized grains, consistent with Regime I grain boundary migration in feldspar. Relict garnet grains and coarse-grained sillimanite porphyroclasts are prevalent, with fractured and boudinaged sillimanite rotated parallel to a well-defined stretching lineation (Fig. 7e). We did not observe any new sillimanite associated with the shear band foliations. As seen on a macroscopic scale, all ductile fabrics in thin section are overprinted by cataclasites and ultracataclasites, and pseudotachylyte veins become numerous as the main thrust contact with the underlying phyllites is approached. Footwall phyllites contain pressure solution bands and quartz grains with deformation bands and occasional sutured grain boundaries (Fig. 7f), indicative of Regime I recrystallization in quartz.
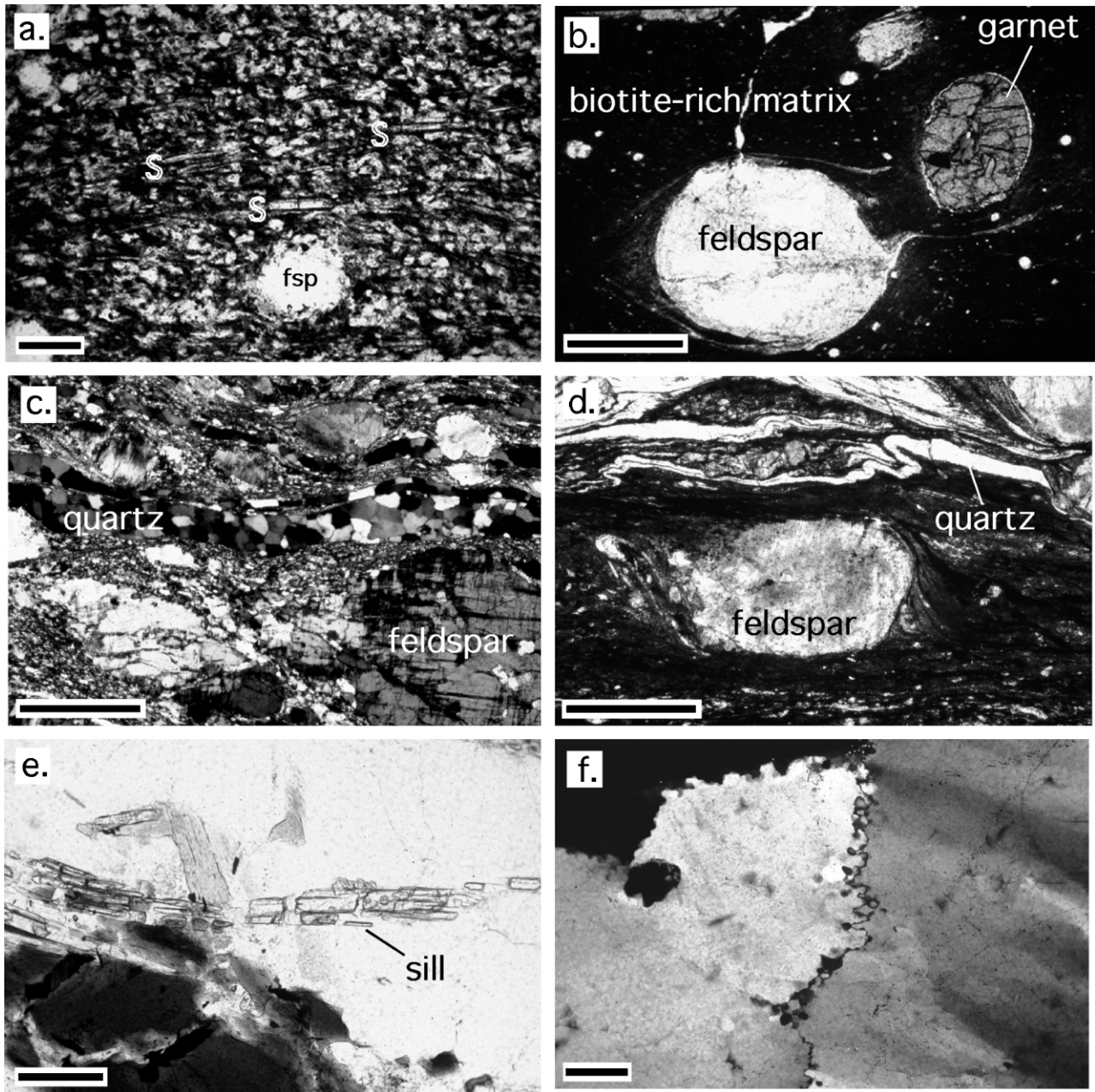
Fig. 7. (a) Syntectonic sillimanite needles (S) define foliation in ultramylonite derived from hanging wall bi-silli-gar gneiss (sample 2 from Fig. 6). Plane light. (b) Delta-type feldspar porphyroclast with tail composed of very fine-grained recrystallized feldspar and quartz + white mica reaction products; from hanging wall ultramylonite. Plane light. (c) Footwall mylonite displaying recrystallized quartz ribbons and coarse feldspar porphyroclasts with tails of very fine-grained recrystallized feldspar. Crossed nicols. (d) Delta-type feldspar porphyroclast and quartz ribbons in a very fine-grained matrix of biotite ± chlorite; from Ambul ultramylonites. Plane light. (e) Boudinaged sillimanite from Los Túneles protomylonites. Plane light. (f) Detail of quartz vein from Los Túneles footwall phyllites, showing deformation bands and sutured grain boundaries. Crossed nicols. Scale bars for (a), (e), (f) = 15 μm; (b), (c), (d) = 100 μm.

5. Discussion

5.1. Strain rates and implications for the brittle–ductile transition

Many of the ultramylonites closest to the hanging wall in the deepest section of the zone, near Merlo, contain syntectonic sillimanite, which indicates deformation temperatures of over 500 °C, at least locally. Although the grain size in the matrix of some of these rocks is a little coarser than is usually associated with ultramylonites, the outcrop, hand specimen, and thin section appearance, with isolated theta- and delta-type porphyroclasts of feldspar and garnet in a uniformly fine-grained biotite-rich matrix, is typical of all ultramylonites. The sub-equant biotite, quartz and feldspar grains and absence of an obvious lattice preferred orientation in the quartz, suggest to us that diffusion-accommodated grain boundary sliding was a significant
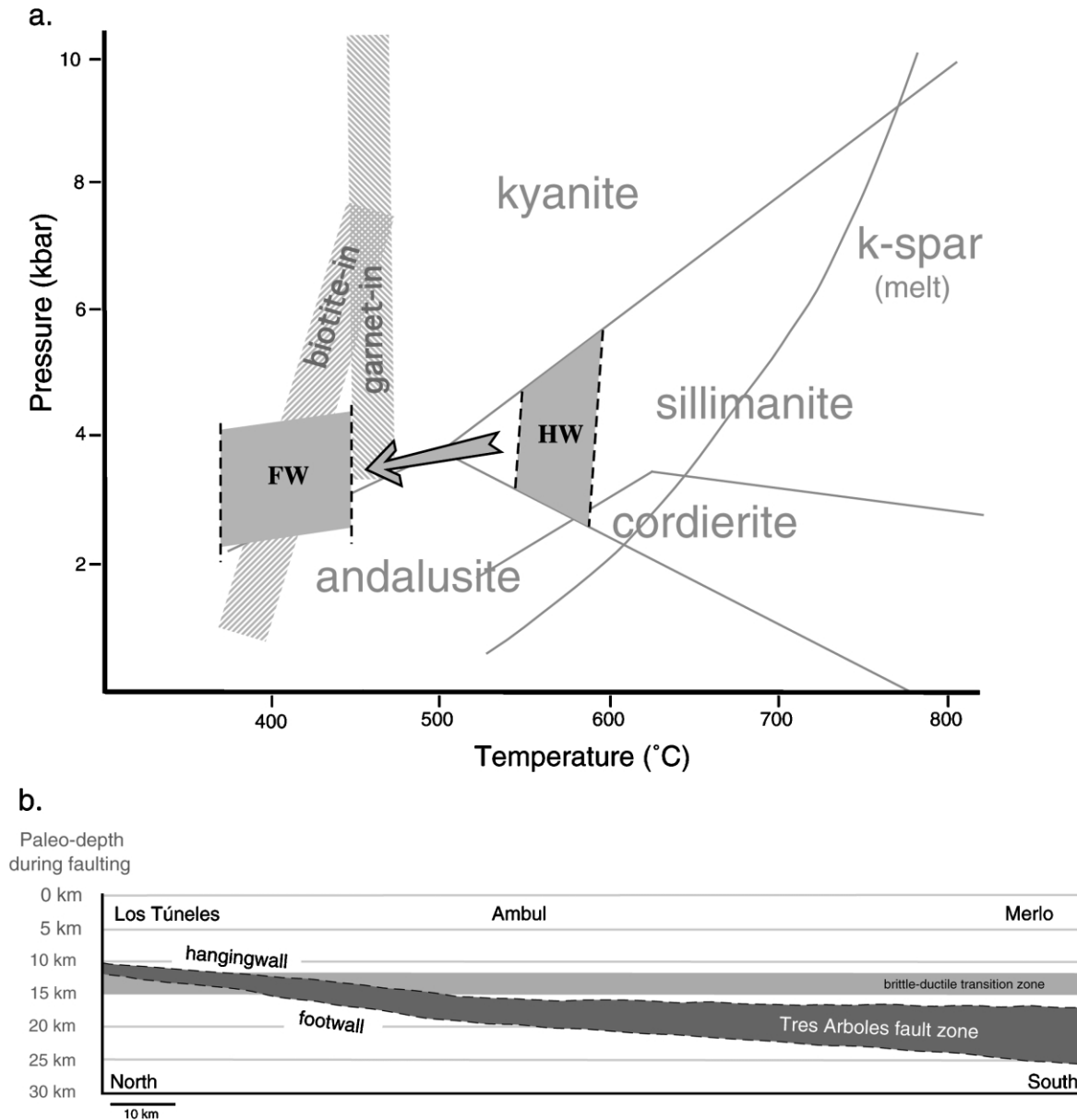
Fig. 8. (a) Probable PT path for rocks of the hanging wall progressing west across the Tres Arboles fault zone in the Merlo region. HW = hanging wall; FW = footwall. (b) Strike-parallel projection of Tres Arboles fault zone before Tertiary uplift and tilting of ranges down to north.

deformation mechanism in these high temperature ultramylonites. The abundance of theta- and delta-type grains in rocks that deformed at temperatures in excess of 500 °C—temperature conditions that would have been conducive to high rates of recrystallization and formation of sigma-type grains at 'normal' strain rates—indicates that strain rates were very fast indeed (Passchier and Simpson, 1986), a conclusion supported by the absence of any pressure shadows around garnet clasts.

In the finer-grained, biotite-rich ultramylonites throughout the main part of the fault zone, from Merlo to Ambul, <5 μm grain sizes in the matrix, weak alignment of biotite and other matrix minerals, sub-spherical garnet clasts with reaction rims of fine-grained quartz, and reaction products of fine-grained white mica and quartz from the breakdown of feldspar, are all indicative of deformation by a combination of reaction softening (Mitra, 1978; White et al., 1980), diffusional mass transfer, and grain boundary sliding (e.g. Boullier and Gueguen, 1975; Allison et al., 1979; Schmid, 1982). Such a combination of mechanisms would be very accommodating of high strain and high strain rates with respect to recrystallization rates, the latter again implied by the presence of numerous theta- and delta-type porphyroclasts in the ultramylonites (Passchier and Simpson, 1986).

The thickness of the high strain zone increases from a maximum of 5 km along the greenschist facies Los Túneles section to 16 km in the high-temperature ultramylonites

near Merlo (Table 1). In Sibson's continental fault zone model and later modifications (Sibson, 1977, 1986; Scholz, 1990), the thickness of ductile shear zones is dependent on strain weakening, which is, in part, dependent on crustal depth. At mid-crustal depths, strain weakening is generally localized along mylonite belts that are tens to hundreds of meters thick (Sibson, 1986). With increased crustal depths, ambient temperatures of quartzo-feldspathic host rocks approach their melting point and migmatites may lubricate the fault zone. This overall weakening of the country rocks facilitates a wider region of strain weakening, and zones of plastically deformed rocks can and do reach thicknesses of 10 km or more (Sorenson, 1983; Hanmer et al., 1995; Hanmer, 2000). We suggest that Sibson's continental fault zone model can be applied directly to the Tres Arboles fault zone, where the narrowest zone of deformation is at the shallowest exposed crustal depths in the northern, Los Túneles section. The dramatic increase in the thickness of the deformation zone to the south correlates with deeper crustal exposures of the fault. Thus, we predict, and observe, a gradual change from brittle–ductile deformation fabrics in the north through greenschist-grade ductile deformation, and finally amphibolite-facies deformation fabrics in the kilometers-wide ultramylonite zone in the south near Merlo. We suggest that similar, very thick zones of ultramylonites may accommodate the high strain rates of many seismically active faults at depths below the brittle–ductile transition.

5.2. Fault displacement estimates

The impressive thickness of ultramylonitic and mylonitic rocks exposed in the Tres Arboles fault zone suggests that there was significant movement along the zone. Direct evidence for the amount of slip is lacking, but an approximate calculation of slip is possible by considering the difference in crustal depth between the hanging wall and footwall and the average dip of foliations within the fault zone. Temperature and pressure conditions of the hanging wall and footwall rocks prior to faulting were deduced from the grade of pre-deformation metamorphism, and mylonite fabrics across the width of the shear zone indicate the temperatures of the rocks during deformation. Assuming a 'typical' range of continental geothermal gradients of 25–30 °C/km, we can estimate the crustal depth ranges of the fault zone rocks at the time of active deformation, and thereby determine the potential displacement of the fault.

Hanging wall rocks proximal to the Merlo region of the Tres Arboles fault zone include sillimanite-grade meta-pelites with interfingered K-feldspar-rich migmatites metamorphosed at temperatures >540 °C (Table 2; Fig. 6). Fabrics within the sheared rocks along the eastern margin of the fault zone include stable, equant sillimanite needles that define the stretching lineation of the mylonites, quartz ribbons consistent with Regime II to III recrystallization and feldspar porphyroclasts with Regime II recrystallized margins, all consistent with ductile shearing at temperatures

>550 °C (Fig. 8a). Assuming a 25–30 °C/km gradient and a minimum temperature of 550 °C, the hanging wall rocks in the Merlo region originated at a depth between 18.5 and 22 km immediately prior to and in the early stages of faulting (Fig. 8b).

Footwall rocks of the Tres Arboles zone near Merlo consist of fine-grained pelites and psammites metamorphosed to a maximum of biotite grade at temperatures between 350 and 450 °C and lack any relict porphyroclasts or fabrics that might indicate retrogression of higher-grade metamorphic minerals. Deformation fabrics from the footwall ultramylonites include quartz grains consistent with Regime II recrystallization and feldspar porphyroclasts with minor grain boundary migration recrystallization and reaction rims of white mica, consistent with deformation at temperatures of 400–450 °C. Granitic mylonites from the footwall contain fractured feldspar porphyroclasts with sutured grain boundaries and quartz textures indicative of Regime II recrystallization, which is also consistent with deformation at temperatures between 400 and 450 °C (Fig. 8a). Depth calculations for the syn-tectonic footwall rocks indicate crustal depths of 13–18 km, which suggests a maximum vertical movement (throw) of 9 km and a minimum throw of 0.5 km for the Merlo region of the fault zone. Combining this vertical estimate with the average 55° dip for shear zone foliations yields a maximum horizontal shortening (heave) estimate of 6 km and a minimum heave of 0.5 km.

Differentiation between hanging wall and footwall rocks within the fault-bounded and retrogressed ultramylonites of the Ambul area is less clear than in the Merlo region. Ultramylonite samples contain relict garnet ± sillimanite, indicating pre-tectonic metamorphism of the hanging wall rocks at temperatures >500 °C, indicating depths of 17–20 km. Quartz deformation fabrics within presumed footwall ultramylonites are consistent with Regime II recrystallization, which suggests deformation at temperatures of 350–400 °C, equivalent to depths of 12–16 km. These temperature estimates suggest a vertical fault movement in the range of 1–8 km and horizontal shortening of 1.5–11 km in the Ambul region. Thus the Ambul section was likely active within a somewhat shallower crustal depth range compared with the Merlo section (Fig. 8b).

In the Los Túneles region, sillimanite + garnet gneisses metamorphosed at minimum temperatures of 500–550 °C are thrust over chlorite grade phyllites. Boudinaged sillimanite prisms in the S fabrics of the S/C mylonites lead us to infer that sillimanite growth was pre-deformation. Syn-tectonic temperatures of 400–450 °C are supported by Regime I recrystallization of feldspar porphyroclasts. Within the footwall rocks, chlorite-grade phyllites contain no evidence for having reached higher grades of metamorphism; pressure solution bands and quartz fabrics indicative of lower Regime I recrystallization suggest shortening at temperatures less than 350 °C. Crustal depth estimates using minimum peak metamorphic temperatures

from the hanging wall rocks and deformation fabrics in the footwall rocks suggest that the Los Túneles hanging wall originated in a depth range of 18–22 km and reached a final depth between 8 and 14 km at the cessation of thrusting. This corresponds to between 6 and 14 km of vertical displacement of the hanging wall—from depths well below the brittle–ductile transition to depths above or within that transition (Fig. 8b)—and the deformation fabrics are consistent with that movement history.

6. Conclusions

The Tres Arboles fault zone is a major, terrane-bounding fault zone that now exposes rocks that deformed over a maximum depth range of 8–22 km. Displacement calculations suggest a vertical movement of 0.5–14 km and a horizontal shortening of 0.5–11 km; the amount of strike slip movement, if any, is presently unconstrained. Deformation conditions show a temperature drop of up to 200 °C from hanging wall to footwall. At its southern and deepest extremity, the fault zone is a 16-km-thick zone of ultramylonite with interspersed mylonite that initially deformed while at sillimanite grade, but that may have been overprinted by lower grade mylonites and ultramylonites as the fault zone developed. Numerous theta- and delta-type feldspar porphyroclasts in a very fine-grained biotite-rich matrix suggest deformation occurred at elevated strain rates, even in the deepest exposed section of the fault zone. Deformation mechanisms included a combination of reaction-enhanced grain size reduction, diffusional mass transfer, and grain boundary sliding.

Exposure of the zone at a shallower crustal level in the north also shows sillimanite-grade gneisses thrust to the west over chlorite-grade phyllites, but here the zone is much narrower and displays shear bands, cataclasites and pseudotachylytes, indicative of deformation at or near the brittle–ductile transition. Our findings are consistent with the crustal fault zone model of Sibson (1977, 1986) and further suggest that the high strain rates of regionally significant, seismically active faults may be accommodated by very thick zones of ultramylonites at depths below the brittle–ductile transition.

Acknowledgements

References

Allison, I., Barnett, R.L., Kerrich, R., 1979. Superplastic flow and changes in crystal chemistry of feldspars. Tectonophysics 53, 41–46.

Bell, T.H., Etheridge, M.A., 1973. Microstructures of mylonites and their descriptive terminology. Lithos 6, 337–348.

Boullier, M.T., Gueguen, Y., 1975. SP-mylonites: origin of some mylonites by superplastic flow. Contributions to Mineralogy and Petrology 50, 93–104.

Camacho, A., Ireland, T.R., 1997. U–Pb geochronology: Final Report. Geoscientific mapping of the Sierras Pampeanas, Argentine–Australian Cooperative Project, Australian Geological Survey Organization, unpublished report.

Cerredo, M.E., 1996. Metamorphic evolution of high grade metapelites of Sierra de Comechingones, Córdoba, Argentina. XIII Congreso Geológico Argentino y III Congreso de Exploración de Hidrocarburos V, 531.

Dalla Salda, L.H., Cingolani, C.A., Varela, R., 1992a. Early Paleozoic orogenic belt of the Andes in southeastern South America: Result of Laurentia–Gondwana collision? Geology 20, 617–620.

Dalla Salda, L.H., Dalziel, I.W.D., Cingolani, C.A., Varela, R., 1992b. Did the Taconic Appalachians continue into South America? Geology 20, 1059–1062.

Dalziel, I.W.D., 1997. Neoproterozoic–Paleozoic geography and tectonics; review, hypothesis, environmental speculation. Geological Society of America Bulletin 109, 16–42.

Dalziel, I.W.D., Dalla Salda, L.H., Gahagan, L.M., 1994. Paleozoic Laurentia–Gondwana interaction and the origin of the Appalachian–Andean mountain system. Geological Society of America Bulletin 106, 243–252.

Davidson, A., 1986. New interpretations of the southwestern Grenville Province. In: Moore, J.M., Davidson, A., Baer, A.J. (Eds.), The Grenville Province. Special Paper Geological Association of Canada 31, pp. 61–74.

Davidson, A., 1990. Two transects across the Grenville Front, Killarney and Tyson Lake areas, Ontario. In: Salisbury, M.H., Fountain, D.M. (Eds.), Exposed Cross-sections of the Continental Crust, Kluwer Academic Publishers, The Netherlands, pp. 343–400.

Dorais, M.J., Lira, R., Chen, Y., Tingey, D., 1997. Origin of biotite–apatite-rich enclaves, Achala Batholith, Argentina. Contributions to Mineralogy and Petrology 130, 31–46.

Gordillo, C.E., 1984. Migmatitas cordieríticas de la Sierras de Córdoba: Condiciones físicas de la migmatización. Boletín de la Academia Nacional de Ciencias, Córdoba 68, 1–40.

Gower, R.J.W., Simpson, C., 1992. Phase boundary mobility in naturally deformed, high-grade quartzofeldspathic rocks; evidence for diffusional creep. Journal of Structural Geology 14, 301–313.

Gromet, L.P., Simpson, C., 1999. Age of the Paso del Carmen pluton and implications for the duration of the Pampean Orogeny, Sierras de Córdoba, Argentina. XIV Congreso Geologico Argentino, Salta I, 149–151.

Gromet, L.P., Simpson, C., Miro, R., Whitmeyer, S.J., 2001. Apparent truncation and juxtaposition of Cambrian and Ordovician arc-accretionary complexes, Eastern Sierras Pampeanas, Argentina. GSA Abstracts with Programs 33, A-155.

Hanmer, S., 2000. Matrix mosaics, brittle deformation, and elongate porphyroclasts: granulite facies microstructures in the Striding–

Athabasca mylonite zone, western Canada. Journal of Structural Geology 22, 947–967.

Hanmer, S., Kopf, C., 1993. The Snowbird tectonic zone in District of Mackenzie, NWT. Geological Survey Paper Canada 93-1C, 41–52.

Hanmer, S., Williams, M., Kopf, C., 1995. Modest movements, spectacular fabrics in an intracontinental deep-crustal strike-slip fault: Striding–Athabasca mylonite zone, NW Canadian Shield. Journal of Structural Geology 17, 493–507.

Hirth, G., Tullis, J., 1992. Dislocation creep regimes in quartz aggregates. Journal of Structural Geology 14, 145–159.

Holdaway, M.J., 2000. Application of new experimental and garnet Margules data to the garnet–biotite geothermometer. American Mineralogist 85, 881–892.

Hooper, R.J., Hatcher, R.D., 1988. Mylonites from the Towaliga fault zone, central Georgia: products of heterogenous non-coaxial deformation. Tectonophysics 152, 1–17.

Jordan, T.E., Allmendinger, R.W., 1986. The Sierras Pampeanas of Argentina: a modern analogue of Rocky Mountain foreland deformation. American Journal of Science 286, 737–764.

Kay, S.M., Gordillo, C.E., 1994. Pocho volcanic rocks and the melting of depleted continental lithosphere above a shallowly dipping subduction zone in the central Andes. Contributions to Mineralogy and Petrology 117, 25–44.

Knipe, R.J., 1989. Deformation mechanisms—recognition from natural tectonites. Journal of Structural Geology 11, 127–146.

Lucero Michaut, N.H., Gamkosian, A., Jarsun, B., Zamora, Y.E., Sigismondi, M., Caminos, R., Miro, R., 1995. Mapa Geológico de la Province de Córdoba, República Argentina, 1:500,000. Ministerio de Economía y Obras y Servicios Públicos. SEGEMAR, Buenos Aires.

Lyons, P., Skirrow, R.G., Stuart-Smith, P.G., 1997. Report on Geology and Metallogeny of the "Sierras Septentrionales" de Córdoba: 1:250,000 map sheet, Province of Córdoba. Geoscientific Mapping of the Sierras Pampeanas. Argentine–Australian Cooperative Project, Australian Geological Survey Organization, unpublished report, 131pp.

Mitra, G., 1978. Ductile deformation zones and mylonites: the mechanical processes involved in the deformation of crystalline basement rocks. American Journal of Science 278, 1057–1084.

Northrup, C.J., Simpson, C., Gromet, L.P., 1998. Early Paleozoic history of the Eastern Pampeanas, Argentina: development of a Cambrian arc and accretionary prism along the margin of Gondwana. X Congreso Latinoamericano de Geología y VI Nacional de Geología Económica II, 400–403.

Otamendi, J.E., Rabbia, O.M., 1996. Petrology of high-grade gneisses from Macizo Rio Santa Rosa: evidence of decompression in the Eastern Sierras Pampeanas. XIII Congreso Geológico Argentino y III Congreso de Exploración de Hidrocarburos V, 527.

Otamendi, J.E., Patiño Douce, A.E., Demichelis, A.H., 1999. Amphibolite to granulite transition in aluminous greywackes from the Sierra de Comechingones, Córdoba, Argentina. Journal of Metamorphic Geology 17, 415–434.

Pankhurst, R.J., Rapela, C.W., Saavedra, J., Baldo, E., Dahlquist, J., Pascua, I., 1996. Sierras de Los Llanos, Malanzan and Chepes: Ordovician I and S-type granitic magmatism in the Famatinian orogen. XIII Congreso Geológico Argentino y III Congreso de Exploración de Hidrocarburos V, 415.

Passchier, C.W., Simpson, C., 1986. Porphyroclast systems as kinematic indicators. Journal of Structural Geology 8, 831–844.

Pérez, M.B., Rapela, C.W., Baldo, E.G., 1996. Geología de los granitoides del sector septentrional de la Sierra Chica de Córdoba. XIII Congreso

Geológico Argentino y III Congreso de Exploración de Hidrocarburos V, 493–505.

Rapela, C.W., Pankhurst, R.J., Casquet, C., Baldo, E., Saavedra, J., Galindo, C., Fanning, C.M., 1998. The Pampean Orogeny of the southern proto-Andes: Cambrian continental collision in the Sierras de Córdoba. In: Pankhurst, R.J., Rapela, C.W. (Eds.), The Proto-Andean Margin of Gondwana. Geological Society, London, Special Publications 142, pp. 181–218.

Rapela, C.W., Pankhurst, R.J., Casquet, C., Baldo, E., Saavedra, J., Galindo, C., 1998b. Early evolution of the Proto-Andean margin of South America. Geology 26, 707–710.

Schmid, S.M., 1982. Microfabric studies as indicators of deformation mechanisms and flow laws operative in mountain building. In: Hsu, K.J., (Ed.), Mountain Building Processes, Academic Press, London, pp. 95–110.

Scholz, C.H., 1990. The Mechanics of Earthquakes and Faulting, Cambridge University Press, Cambridge, p. 439.

Sibson, R.H., 1977. Fault rocks and fault mechanisms. Journal of the Geological Society of London 133, 191–213.

Sibson, R.H., 1986. Earthquakes and rock deformation in crustal fault zones. Annual Review of Earth and Planetary Sciences 14, 149–175.

Simpson, C., Whitmeyer, S.J., De Paor, D.G., Gromet, L.P., Miro, R., Krol, M.A., Short, H., 2001. Sequential ductile through brittle reactivation of major fault zones along the accretionary margin of Gondwana in Central Argentina. In: Holdsworth, R.E., Strachan, R.A., Macloughlin, J.F., Knipe, R.J. (Eds.), The Nature and Tectonic Significance of Fault Zone Weakening. Geological Society, London, Special Publications 186, pp. 233–254.

Sims, J., Stuart-Smith, P., Lyons, P., Skirrow, R., 1997. Informe geológico y metalogénico de Las Sierras de San Luis y Comechingones, Provincias de San Luis y Córdoba. Argentine–Australian Cooperative Project, Australian Geological Survey Organization, unpublished report, 148pp.

Sims, J., Ireland, T.R., Camacho, A., Lyons, P., Pieters, P.E., Skirrow, R., Stuart-Smith, P., Miro, R., 1998. U–Pb, Th–Pb and Ar–Ar geochronology from the Southern Sierras Pampeanas, Argentina: implications for the Paleozoic tectonic evolution of the western Gondwana margin. In: Pankhurst, R.J., Rapela, D.W. (Eds.), The Proto-Andean Margin of Gondwana. Geological Society, London, Special Publications 142, pp. 259–281.

Sorenson, K., 1983. Growth and dynamics of the Nordre Stromfjord shear zone. Journal of Geophysical Research 88, 3419–3437.

Stuart-Smith, P.G., Miró, R., Sims, J.P., Pieters, P.E., Lyons, P., Camacho, A., Skirrow, R.G., Black, L.P., 1999. Uranium–lead dating of felsic magmatic cycles in the southern Sierras Pampeanas, Argentina: implications for the tectonic development of the proto-Andean Gondwana margin. In: Ramos, V.A., Keppie, J.D. (Eds.), Laurentia–Gondwana Connections before Pangea. Geological Society of America Special Paper 336, pp. 87–114.

Tullis, J.A., 1977. Preferred orientation of quartz produced by slip during plane strain. Tectonophysics 39, 87–102.

Von Gosen, W., Loske, W., Prozzi, C., 2002. New isotopic dating of intrusive rocks in the Sierra de San Luis (Argentina): implications for the geodynamic history of the Eastern Sierras Pampeanas. Journal of South American Earth Sciences 15, 237–250.

White, S.H., Burrows, S.E., Carreras, J., Shaw, N.D., Humphreys, F.J., 1980. On mylonites in ductile shear zones. Journal of Structural Geology 2, 175–187.